Influence of Visual and Haptic Feedback on the Detection of Threshold Forces in a Surgical Grasping Task

John-John Cabibihan ⬡, Ahmad Yaser Alhaddad ⬡, Tauseef Gulrez ⬡, and W. Jong Yoon ⬡

Abstract—**Feedback from sensory modalities is crucial for the precise grasping of tissues during minimally invasive robotic surgery. The aims of the study are to determine the influence of visual and haptic feedback on the detection of threshold forces and to evaluate the applicability of the sensory integration model to a surgical grasping task. A sensorized surgical grasper and a fingertip haptic force feedback device were used. Three types of stimuli were presented (i.e. visual-alone, haptic-alone, and bimodal visual and haptic stimuli). Threshold forces of 100 mN and 87.5 mN were detected for visual and haptic feedback, respectively. When bimodal feedback was provided, the participants detected a threshold force of 75 mN. The threshold force for the bimodal condition was 28.6% lower than the visual-alone feedback and 15.4% lower than the haptic-alone feedback stimuli. Our bimodal condition results showed that there was a 13.1% difference between the experimental result and the predicted value from the sensory integration model. The threshold force discrimination was strongly influenced by the haptic force feedback. It is likely that the tissue stiffness can be more intuitively perceived through the direct force stimulation of the fingertip than just by visual observation alone. Cues like small deformations or changes in the grasping angles of the surgical tool are more difficult to interpret visually as compared to the haptic modality.**

Index Terms—**Force and tactile sensing, grasping, haptics and haptic interfaces, laparoscopy, surgical robotics.**

I. INTRODUCTION

MINIMALLY invasive surgery is getting more preferred over the traditional open surgery procedures due to its significant benefits for patients. Minimally invasive surgery requires less incisions; therefore, it has less risk of infection, less pain, and faster recovery [1]. However, there are remaining

challenges associated with minimally invasive surgery, such as the impaired perception of depth, lack of feedback for soft tissue palpation, and the limited view of the operative field [2]. In the classical work of Posner *et al.* [3], they have regarded visual cues as superior to other feedback cues in terms of perceptual accuracy, memory recall, and speed of response. More recently, the importance of haptic feedback has been considered to overcome the issue of the loss of force feedback in robotic surgery [4]. Laparoscopic grasping tasks are examples of procedures that require the delicate manipulation of soft tissue [5]. Surgical sutures (i.e. diameter of less than 0.7 mm) also require careful manipulation of the surgical grasper at small angles to prevent tissue damage and suture breakage due to high grasping forces and excessive pulling [6], [7]. It has been recognized that the lack of haptic feedback system resulted in soft tissue damage and harm from excessively tight or loose stitches [6].

Previous studies demonstrated the promising potential of haptic devices in surgical tasks and in robotic assisted surgeries [8], [9]. Park *et al.* [10] investigated the utility of haptic feedback in delivering the appropriate perceived difference between two close presentations of a stimuli. They investigated the accuracy of the perceived sharpness of haptic edges between real and virtual environments. In that study, the participants were asked to match the sharpness of virtual edges to that of real edges. Yoon *et al.* [11] investigated the perceived curvature of virtual surfaces. The participants were presented with two virtual sequential concave surfaces and were asked to discern the surface with the higher curvature. To date, limited studies were conducted to evaluate the efficacy of a haptic system in improving the perceptual capabilities of a user in evaluating between two subsequent presentations of grasping forces in surgical robotic tasks.

It was hypothesized that when humans integrate visual and haptic information, the combined estimates should have lower discrimination thresholds than either the thresholds from visual or haptic estimates alone. This is represented by the sensory integration model of Ernst and Banks [12]:

$$T_B = \sqrt{\frac{T_V^2 \cdot T_H^2}{T_V^2 + T_H^2}} \tag{1}$$

where T_V, T_H, and T_B are the threshold forces for visual-alone, haptic-alone, and bimodal feedback, respectively. In the original experiments [12], the participants were asked to judge the sizes

of two bars, which were sequentially presented in a visual-alone and haptic-alone experimental paradigm. The objects' sizes were judged as finer when visual and haptic inputs were integrated than when vision or haptic inputs were independently provided. In this letter, we ask whether the same principle applies to force threshold perception.

This letter has two aims. First, we investigate the influence of visual and haptic feedback on the detection of threshold forces (i.e. just noticeable difference (JND)) in a surgical grasping task. Second, we examine whether the sensory integration model applies to the perception of threshold forces. In achieving those aims, the following are the contributions of this work:

1) A surgical grasper was described and characterized for a small span of grasping angles (i.e. 18.5°–21.5° grasp angles for a 3° span). Delicate suturing and manipulation of soft tissue are characterized by small changes in grasping angles.

2) A single-button indenter haptic device was designed and characterized for low-force indentation (i.e. 0-500 mN). This patented device can be mounted on the stylus of a commercial haptic device.

3) We showed that haptic feedback has a stronger influence than visual feedback in the detection of threshold forces. Visual feedback allows faster convergence, but the threshold forces are higher.

4) We demonstrate that our results were aligned with the sensory integration model [12] but has some limitations on the perception of threshold forces.

This letter is organized as follows. Section II describes the design and characterization of the grasper and the haptic device. Section III describes the experiments to determine the force thresholds. Section IV provides the results and Section V discusses the results. Finally, Section VI concludes the study.

II. DESIGN AND CHARACTERIZATION

A. System Design Overview

The surgical robotic grasping system in our study provided haptic and visual feedback to the user (Fig. 1). The haptic force feedback to the user's fingertip was provided by an indenter while the visual feedback was presented through a display system that showed the grasping tasks on a soft tissue.

B. Surgical Grasper

1) Design: A surgical grasper (Fig. 2(a)) was used for the experiments. It was designed for laparoscopic surgery research and was evaluated for its reliability in [13]. The grasper operates with a cable-driven mechanism. A servo motor was connected to the driving pulley with a gear system to control the pulley's rotation. A schematic of the grasper's driving mechanism is shown in Fig. 2(b). The grasping force, f_{grasp}, is applied to the tip through the cables and can be calculated with the relationship below:

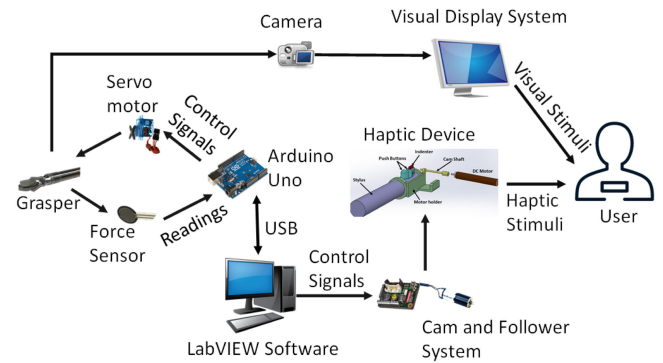$$f_{grasp} = \frac{r_1}{r_2 \, l} \left(T_{upper} + T_{lower} \right) \qquad (2)$$

Fig. 1. System design overview. The grasper was equipped with a force sensor that sensed the applied force on a tissue. The grasper was controlled by a servo motor. Both the force sensor and the servo motor were interfaced to a computer system through a microcontroller. The grasping forces were mapped to the indentation levels on the haptic device. A video camera displayed the visual stimuli on a dedicated screen to the user. A script handled the coordination of all components in the system.
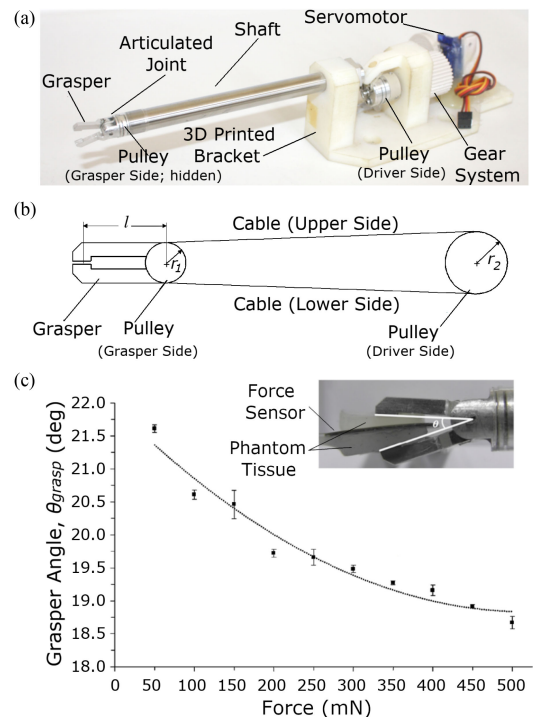

Fig. 2. The surgical grasper components and characterization. (a) Detailed components of the surgical grasper. (b) Schematic of the grasper's mechanism. (c) Characterization of the grasping angle vs force for the phantom soft tissue. The grasping force readings were from 50 mN to 500 mN, with an increment value of 50 mN. The grasping force was obtained from a force sensor that was embedded between 2 layers of phantom tissues with 3 mm layer thickness. The grasping angle, θ_{grasp}, was obtained through image processing. The error bars show the standard error of the mean (SEM). The coefficient of determination, R^2, was 0.96.

where r_1 is the radius of the driven pulley nearest to the grasper and r_2 is the radius of the driver pulley. The length, l, is the distance from the grasper's hinge to the grasper's tip. T_{upper} and T_{lower} represent the torque values from the upper and lower sides of the cable.
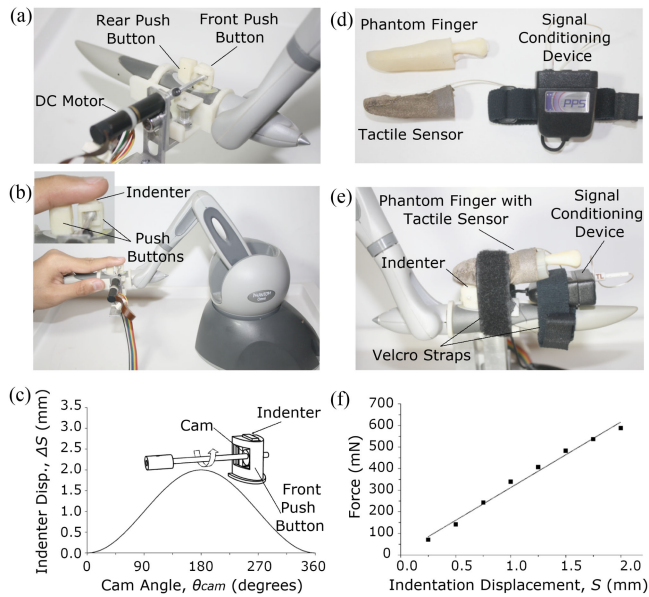
Fig. 3. The developed force feedback device mounted on the stylus of the Geomagic Touch Haptic Device and characterization of the haptic device. (a) Detailed components of the force feedback device. (b) A subject's finger resting on the push button of the force feedback device. The inset shows the indenter providing contact to the fingertip. (c) Profile of the indenter's displacement, ΔS, as a function of the cam angle, θ_{cam}. (d) The phantom finger and the tactile sensor connected to the signal conditioning device. (e) The tactile force sensor worn over the phantom finger. The finger was fixed to the indenter using velcro straps. (f) The contact force vs displacement of the indenter obtained a coefficient of determination, R^2, of 0.99.

2) Characterization: The grasper was characterized to obtain the relationship between the grasping force and the grasping angle. A force sensor (B201, FlexiForce Force Sensor, Tekscan Inc, USA) was used to measure the grasping force (Fig. 2(c)). The sensor was embedded between two layers of soft silicone material (Ecoflex OO-30, Smooth-On Inc, USA), each with 3 mm thickness. The soft material was casted on a $15 \times 15 \times 3$ mm^3 mould. This material was used as a phantom heart, breast or prostate tissue in earlier works [14], [15]. The grasper was programmed to grasp the sample with a 1 sec ramp loading, 5 sec hold, and a 1 sec unloading [16], and with 1 minute interval to recover [17]. The grasping angle and the grasping force were characterized (Fig. 2(c)). The following second-order curve was fitted to the experimental data:

$$\theta_{grasp} = 11.4F^2 - 11.94F + 21.93 \qquad (3)$$

where θ_{grasp} is the measured grasping angle and F is the grasping force obtained from the sensor.

C. Haptic Force Feedback Device

1) Design: To provide tactile force feedback on the fingertip, a haptic device (Fig. 3(a)) was designed to deliver feedback on the fingertip through a single-button indenter [18]. The device was designed to be mounted on the stylus of a commercially-available haptic device (Geomagic Touch Haptic Device, 3D Systems, USA), which is widely-used in haptics research (e.g. [19], [20]). The device has two built-in push

buttons (Fig. 3(a)). The front push button is for closing the grasper, while the rear push button is for opening the grasper. So as not to lose these functionalities, the force feedback indenter was constructed using a 3D printed structure with a 10 mm height for the index finger to rest on (Fig. 3(b)). The indenter has a 4×2 mm^2 surface contact area to provide force feedback on the distal phalange of the index finger at the site near the papillary whorl. Preliminary evaluation of the device's reliability was reported in [18].

A cam and follower mechanism (Fig. 3(b) and Fig. 3(c) inset) was used to transform the rotary motion from the motor to a vertical displacement movement of the indenter. A geared DC motor (part number 345879, Maxon Motor AG, Switzerland; 256:1 gear ratio) was used to drive the cam shaft (Fig. 3(c)). The angular position was determined through an encoder (Encoder MR, Maxon Motor AG, Switzerland; with 128 ticks/revolution resolution). A Labview-based script controlled the velocity and position of the indenter using a proportional-integral-derivative (PID) controller operating at 5 kHz. The indenter was situated inside the front push button structure, which enabled a vertical translation from 0 to 2 mm. The indenter was designed to follow a simple harmonic motion curve using (4). The change in the displacement of the indenter, ΔS, in relation to the rotation of the cam, θ_{cam}, was defined as:

$$\Delta S = \frac{H}{2} \left[1 - \cos \frac{\pi \theta_{cam}}{\beta} \right] \qquad (4)$$

where H is the vertical rise of the follower (i.e. 2 mm) and β is the rotation angle at which the follower reaches the maximum height (i.e. 180°). In this case, the height of 2 mm indentation displacement will be achieved with a 180° rotation angle of the cam. The indentation of the haptic device on the fingertip varies as the cam rotates with various angles, θ_{cam}, in accordance to the motor's rotation (Fig. 3(c)).

2) Characterization: The device was characterized to obtain the relationship between the contact force and the indentation displacement. In pilot tests, unnecessary finger or hand movements caused a disturbance in the sensor readings. To get consistent force versus indentation measurements, a phantom finger was made to wear the tactile sensor. The protocol using phantom fingers was similar to the experimental characterization setup in McKinley *et al.* [21].

The sensor (FingerTPS, Pressure Profile Systems, USA) is made of tactile pads that detect changes in capacitance when the upper and lower tactile pads come into contact. This sensor was previously used to characterize the grasping forces of human and prosthetic hands [22]. The sensor was selected due to its thin profile (2 mm), applicable force range (0-19.6 N), linearity (99%), and repeatability error (1%). The sensors were connected to a signal conditioning device. The sample rate was 40 Hz. The sensor readings were recorded by a sensor data analysis software (Chameleon, Pressure Profile Systems, USA).

The phantom finger in Fig. 3(d) was obtained from an earlier experimental work of Cabibihan *et al.* (cf. Fig. 9 in [23]) where this section of the finger was found to have a similar skin compliance as that of a human finger (i.e. a 1 N indentation force corresponds to 1-2 mm skin displacement). The phantom finger
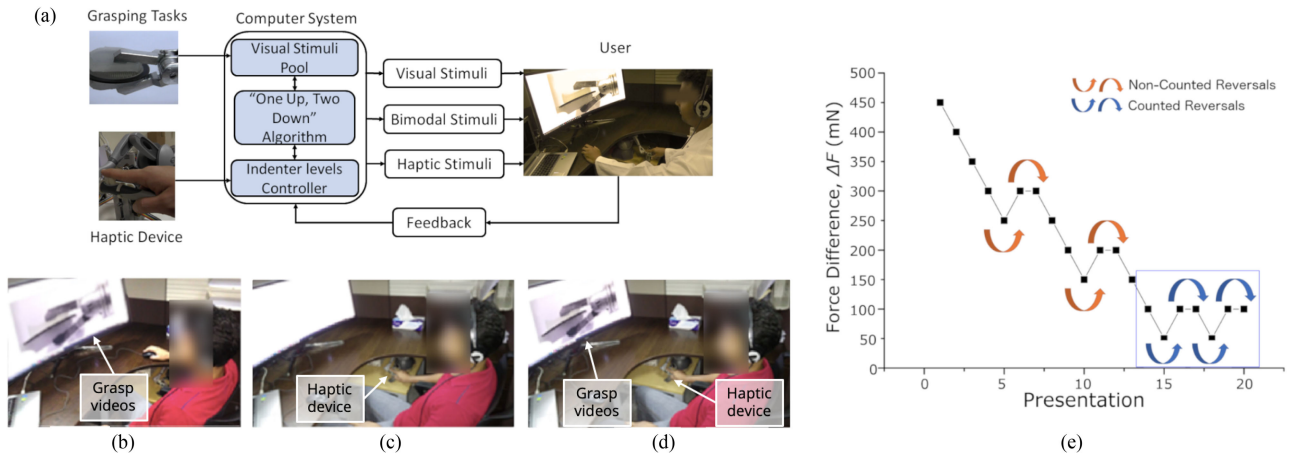
Fig. 4. Overview of the experimental design. (a) The grasping tasks on a phantom soft tissue was shown as videos. The haptic device provided force feedback. The computer system coordinated all the components of the system, arranged the presentations according to feedback from the user, and provided the stimuli to the user. Presentation of the stimuli was counterbalanced across participants. (b) Visual-alone. (c) Haptic-alone. (d) Bimodal visual and haptic stimuli. For the purpose of showing the location of the haptic device, the curtain to cover the hand of the participant was removed. (e) A sample result from one of the participants. The algorithm counted up to 8 reversals before it terminated. From the last 4 reversals (boxed), the mean value of the force difference, ΔF, was calculated and was used for the analysis.

was constructed from the computed tomography (CT) data of a subject's right index finger using techniques described in earlier works [23], [24]. From the CT data, the bone structure and the external surface of the finger were 3D printed (Replicator 5th Generation, MakerBot Industries LLC, Brooklyn, NY, USA). The artificial skin was casted with a soft material (Ecoflex OO-30, Smooth-On Inc, USA) similar to the phantom tissue in Fig. 2(c). The same material was extensively used in soft prosthetic and robotic fingers [25], [26]. Considering that the maximum force in surgical graspers from an earlier work [13] was within 0 to 500 mN, this force range needs to be mapped to the indenter's displacement of 0 to 2 mm (see Section II.B.2).

The phantom finger was then fixed over the indenter using velcro straps (Fig. 3(e)). The indenter was controlled using a script (LabVIEW VI, National Instruments, Austin, TX, USA) to perform the $180°$ rotation of the cam shaft, which then corresponded to changes in the indentation displacements from 0 mm to 2 mm, with increment value of 0.2 mm. As the cam rotated, the changes in the indentation forces were recorded. Fig. 3(f) shows the relationship between the indenter's displacement and the contact force recorded at the phantom fingertip. The following equation was fitted to the experimental data:

$$F = 0.3038S + 0.0091 \tag{5}$$

where F is the contact force on the fingertip and S is the indentation displacement applied by the haptic device to the fingertip.

III. PERCEPTUAL EXPERIMENTS

A. Participants

Sixty subjects (38 males, 22 females, 22-42 years old) took part in the experiments. All participants were healthy volunteers and had normal or corrected-to-normal vision and normal touch. The procedures did not include invasive or potentially dangerous

methods and were in accordance with the Code of Ethics of the World Medical Association (Declaration of Helsinki). Data were stored and analyzed anonymously. All participants gave their written informed consent.

B. Stimuli

The participants were presented three types of stimuli (Fig. 4(a); video link). The visual stimulus was a set of video recordings of grasping tasks at different force levels. The haptic stimulus was force feedback from the indenter device to the user's fingertip. The bimodal stimuli combined both the visual and haptic feedback. The participants were asked to be seated in front of a 35 in LCD monitor (model XR3501, BenQ Corp, Taiwan). The haptic device was positioned within the reach of the participant's right hand and was covered with a curtain. To filter out the sound emitted by the motor and other ambient sounds, the participants wore a headphone that played white noise.

For the visual-alone stimulus (Fig. 4(b)), ten videos of the surgical grasper were taken as it grasps the phantom tissue at different grasping forces. The grasping forces were from 50 mN to 500 mN. In microneurosurgery [27], it was reported that the median forces in sharp dissection was 30 mN. For blunt dissection, the median forces were 220 mN. An incremental value of 50 mN was considered to cover the range of grasping forces (i.e., up to 500 mN) in consideration of the median forces exerted during sharp and blunt dissections.

During an experiment, two consecutive videos were presented in sequence. The time gap between the presentation of the two videos was 3 section The order of the videos was randomized, but was kept at a certain force difference. This force difference is decreasing or increasing depending on the responses of the participants. After the two videos were shown, a window pops up that asks the question: "Which of the two forces is higher?". With a computer mouse, the participants will then select a button

---

Algorithm 1: One-Up, Two Down Pseudocode.

Input: User's answer
Output: Visual and/or haptic stimuli
1 **while** *(Num. of iterations < 50) and (Num. of reversals < 8)* **do**
2   Display two stimuli (i.e. presentation) and wait for the user's answer
3   **if** *Answer is correct* **then**
4   Check previous answer
5   **if** *Correct* **then**
6   Decrease stimuli difference by one increment
7   **else if** *Incorrect* **then**
8   Keep the current stimuli difference
9   **else if** *Answer is incorrect* **then**
10   Increase the stimuli difference by one increment
11   Check for reversal
12   **if** *Reversal is detected* **then**
13   Increase Num. of reversals
14   Increase Num. of iterations

---

on the monitor that shows: "First" or the "Second". Henceforth, the term "presentation" will be used to describe the display of a pair of stimuli to be compared.

For the haptic-alone stimulus (Fig. 4(c)), ten different indentation levels were used in the program to present the force values on the index finger through the haptic feedback device. The indentation displacements were from 0 to 2 mm at 0.2 mm increments, which corresponded to grasping force values of 50 to 500 mN at 50 mN increments. During the experiments, two consecutive haptic indentations were done on the fingertip. Similar to the visual-alone experiment, the order was randomized, but was kept at a certain indentation difference that changes depending on the participant's answers. Additionally, the gap between the two presentation of indention was 3 section The procedure to make a selection was also similar to the visual-alone experiments.

For the bimodal visual and haptic stimuli (Fig. 4(d)), the presentations for the visual and haptic stimuli were synchronised in terms of force values and timing. Likewise, the participants were made to select the higher force value between the two sets of stimuli that were presented.

C. Algorithm

To determine the smallest perceivable force difference between a higher and a lower force, an adaptive algorithm known as the "one up, two down" algorithm [28] was used in the experiments. The algorithm calculated the difference in force values between the participant's current and previous answer, which was then stored as the force difference, ΔF. For us to determine whether the participant was certain of his/her choice, the program tracked the reversals (i.e. number of sign changes) of the ΔF. Algorithm 1 shows the pseudocode for the one up, two down algorithm. To further illustrate the algorithm, please refer to a sample result from one of the participants (Fig. 4(e)).

D. Experimental Design and Data Analysis

Before an experiment, the participant was shown the set-up. There was a 10-minute training period before the experiments for the participants to gain familiarity with the stimuli and the procedure. The order of presentation of the stimuli was counterbalanced across participants using Latin squares. The

Shapiro-Wilk test was used to determine if the datasets associated with the threshold and presentation were normally distributed. The datasets did not pass that test. A Kruskal-Wallis test, a nonparametric version of the one-way ANOVA, was used on the data. If statistical significance was found, Mann-Whitney test with Bonferroni correction was used to compare the pairs of stimuli groups. Because the distributions were skewed, the results were reported as median and not as the mean and standard deviation. The statistical analysis software package OriginPro was used for the analysis (v2016, OriginLab Corp., MA, USA). Statistical significance was set to $p < 0.05$. The datasets are available at IEEE DataPort [29].

IV. RESULTS

The participants' task was to identify the threshold forces in a visual-alone, haptic-alone, and combined visual and haptic feedback paradigm. Fig. 5 shows the convergence of the forces from the participants' responses. It can be observed that the variance in the visual-alone results are higher than the haptic-alone or bimodal feedback results.

Fig. 6(a) shows the detection threshold forces. A Kruskal-Wallis test showed that the perception of threshold forces were significantly affected by the type of stimuli, $H(2) = 33.37$, $p < 0.0001$. Post-hoc Mann-Whitney tests using a Bonferroni-adjusted alpha level of 0.017 (0.05/3) were used to compare all the pairs of groups. The threshold forces for visual feedback (*Median* = 100 mN) was significantly different from haptic feedback (*Median* = 87.5 mN), $U = 2722.5, z = 4.98, p < 0.001$. Likewise, the threshold for visual feedback (*Median* = 100 mN) was higher than the bimodal feedback (*Median* = 75 mN), $U = 2703.5, z = 4.89, p < 0.001$. No significant differences were found between haptic (*Median* = 87.5 mN) and bimodal (*Median* = 75 mN) feedback, $U = 1768, z = -0.18, p = 0.86$. These results indicate that the participants perceived the lower threshold forces better in both the haptic and bimodal feedback as compared to visual feedback.

To determine which stimulus converges faster to reach the detection thresholds, we collected the number of iterations that took each participant to complete the task (Fig. 6(b)). The feedback modality had a significant effect as shown by the Kruskal-Wallis test, $H(2) = 18.14, p < 0.001$. Mann-Whitney tests with Bonferonni correction at the 0.017 level were used for comparing all pairs of stimuli. The number of presentations for the visual feedback (*Median* = 27) was significantly different from haptic feedback (*Median* = 31), $U = 1122.5, z = -3.56, p < 0.001$. The visual feedback (*Median* = 27) was also significantly different from the bimodal feedback (*Median* = 32), $U = 1078, z = -3.79, p < 0.001$. The haptic and the bimodal feedback were not found to be significantly different, $U = 1759, z = -0.21, p = 0.83$. This result is in agreement with Posner *et al.* [3], who suggested that vision is more dominant over haptics in terms of the speed of response when perceptual judgements were required from human observers.

According to the hypothesis of Ernst and Banks [12], the integration of both visual and haptic stimuli results to lower
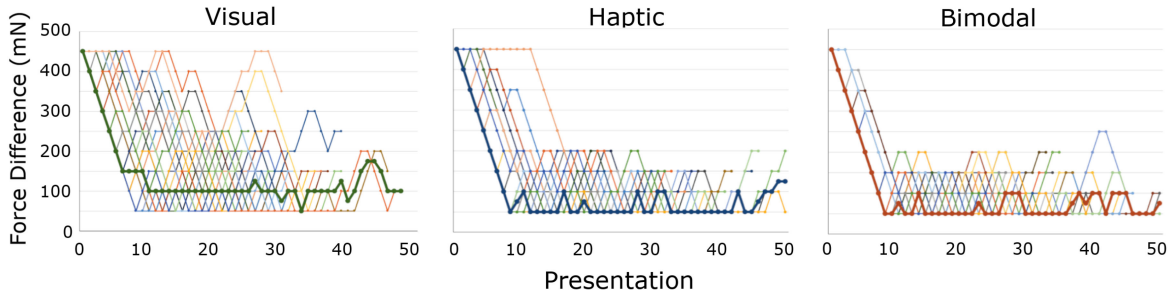
Fig. 5. The convergence of the perception of threshold forces by the participants in the experiment. There is a large variance in the visual stimulus as compared to the haptic and bimodal stimuli. Bold lines show the median values for each presentation iteration.
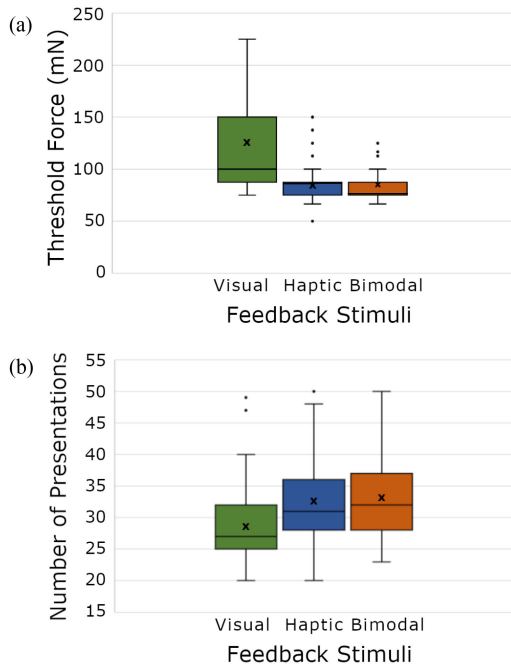

Fig. 6. Threshold forces and number of presentations. (a) Threshold forces for the visual, haptic, and bimodal feedback modalities. (b) The number of presentations before reaching the threshold force perception. Horizontal bars inside the box indicate the median, the X marks indicate the mean, box edges are the 25th and 75th percentiles, the whiskers indicate range, and dots denote outliers.

TABLE I
EXPERIMENTAL AND PREDICTED THRESHOLD FORCES (MN)

T_V(Expt)	T_H(Expt)	T_B(Expt)	T_B(Predicted)
100	87.5	75	65.8

thresholds than either visual or haptic feedback can independently provide. We calculated the combined threshold forces according to (1). The predicted bimodal threshold force was 65.8 mN while our experimental result with bimodal feedback was 75 mN, corresponding to a 13% difference (Table I).

V. DISCUSSION

A. Haptic Feedback is More Dominant on Force Threshold Detection, But Visual Feedback Converges Faster

We presented the design and characterization of a sensorized surgical grasping tool and a patented single indenter haptic mechanism [18]. The haptic mechanism has a simple construction and latches on to the stylus of a widely-used haptic feedback device. The experimental results showed that participants can discriminate threshold forces of 87.5 mN with haptic feedback and 75 mN with bimodal feedback. Both of which were more sensitive than the threshold forces of 100 mN achieved with visual feedback alone. Visual-alone feedback allowed a faster convergence (27 presentations) to the threshold force, but the threshold force was perceived at higher values. The participants completed the visual-alone presentations faster but this did not mean that their responses corresponded to the appropriate threshold forces. Haptic feedback allowed a slower convergence (31 presentations), but the perceived threshold force was lower. When bimodal feedback stimuli were presented to the participants, the threshold force was 28.6% lower than the visual feedback stimulus. Moreover, it took the participants around 32 presentations to determine the threshold force with bimodal feedback, which was closer to the results of the haptic feedback (31 presentations). The results for the bimodal feedback had 15.4% difference with the results of the haptic feedback in force thresholds and 3.2% difference in the number of presentations to reach the threshold. Participants appeared to have relied more on the haptic feedback cues than the visual cues during the grasp experiments for a small span of angles (i.e. $< 3°$).

B. Visual Feedback Alone is Not Enough

The participants had more difficulty in detecting the differences in threshold forces from the observation of tissue deformation or the increase or decrease in grasping angles. Fig. 2(c) shows that grasping angles from 18.5° to 21.5° correspond to 0-500 mN grasping forces in the surgical tool. The 3° operating span for the 0-500 mN applied forces can represent surgical operations that require small changes in grasping angles (e.g. laparoscopic grasping of tissues [30], minimally invasive suturing and knot tying [31]).

The phantom tissue that we used in the experiments has similar mechanical characteristics to human fingertip tissues [21], [23]. The mechanical behavior consists of hyperelastic and viscoelastic behaviors where the application of forces do not correspond to linear increase or decrease in displacement [32]. Moreover, there can be differences in the stiffness of internal organs across different patients [33]. These make the perceptual estimation of forces by visual means a difficult task. There are several experimental robotic systems that have haptic feedback, yet the most advanced robotic surgical systems only have vision-based monitors for surgical procedures so far [34].

From a surgeon's console of a robot surgical system, the monitor displays high definition views of the surgical site. These views have a variety of optical interactions like specular reflections, partial occlusions, body fluids, and shadows [35]. If the useful visual cues were affected by any of these, our results indicate that the perceptual detection of force changes during an operation need to be further improved. We showed that the combined visuohaptic threshold force was closer to the haptic-only threshold force than to the visual-only threshold force. While it can be argued that visual feedback from an endoscopic camera does not have to deal with the latencies from processing tactile sensor signals at the grasping tooltip and presenting the corresponding force to the user's fingertip, there is a marked advantage of having redundant information from the additional haptic modality. When visual and haptic stimuli were combined, the threshold forces were lower than having visual cues alone. It remains to be understood whether the participants relied mostly on the haptic feedback during the bimodal experiments or to the proportion to which visual feedback contributed to the threshold force detection during the bimodal feedback experiment.

C. Limitation of the Sensory Integration Model

It was hypothesized that the combined estimates from visual and haptic information would result into lower discrimination thresholds than either the thresholds from single modality alone ([12]; (1)). Our results were in alignment with that hypothesis although the experimental result for the bimodal feedback (i.e. 75 mN) had a 13.1% difference from the predicted results when visual and haptic feedback were combined (i.e. 65.8 mN).

In our experiments, the stiffness of the phantom tissue may have played a role in the results. The haptic information appears to have dominated the perceptual estimate because the force-displacement mapping on the fingertip was linear (Fig. 3(f)) and it could be more intuitive to interpret. For the visual feedback, the mapping of the force and grasping angle showed a non-linear behavior (Fig. 2(b)), which might be more difficult to interpret. In a future experiment, participants may need to be given more time to actively explore the stiffness of the phantom tissue by letting them palpate the tissue with the grasping tool. In doing so, this can give them time to develop strategies in dealing with the non-linear behavior of soft tissues. Active exploration of an object is one of the strategies for understanding object properties, such as hardness, shape, texture, and weight [36].

An alternative to the sensory integration model [37], [38] suggested that to achieve a coherent perception, the estimates need to include other object properties (e.g object stiffness, surface texture) and derive signal-specific estimates for the property from each signal. All these estimates will then have to be combined by weighted averaging. It was further suggested that material properties, such as friction and compliance, were additional factors in order to achieve more reliable perceptual estimates [37], [39].

D. Limitations and Future Work

The investigation in this letter was limited to a single-indenter haptic force feedback system. A multi-modal feedback system could be considered to investigate different stimulation modalities [40]. Additionally, the vertical translation of the indenter was limited to 2 mm. Higher indentation displacements could be considered to reflect a larger force range or to provide higher resolution for the mapping of the forces involved using haptic arrays.

In our study, the mapped range of force was limited to 500 mN. However, in an actual surgery, the mapping of the haptic device will be set based on the tissue of interest and the acceptable working range of forces. For example, the maximum allowable grasping force will be mapped to the maximum indentation level of the haptic device. Through this, a more adaptive mapping of forces can be achieved. Furthermore, the exact thickness and tissue moisture need to be considered [41]. Future work can also consider the use of tissues from animal or human organs for the grasper to operate on so that the participants can gain more insight in the estimation of forces through visual cues from soft material deformations. The training effects or the long term usage of the developed haptic feedback system were not investigated in this study. The participants in the study did not have tactile or visual impairments, but they were not trained surgeons.

VI. Conclusion

Vision and touch through haptic perception offer advantages and limitations for robotic surgery. Vision depends on cues that can be observed from the monitor, whereas haptic perception depends on the direct contact of the fingertip with a force feedback device. We demonstrated that a single-indenter haptic feedback mechanism can strongly influence the detection of threshold forces in a surgical grasping task. Such findings have implications for the predominantly visual-based feedback systems of surgical robots that are being developed.

REFERENCES

[1] J. Máca *et al.*, "Surgical injury: Comparing open surgery and laparoscopy by markers of tissue damage," *Therapeutics Clin. Risk Manage.*, vol. 14, pp. 999–1006, 2018.

[2] J. Marescaux and M. Diana, "Next step in minimally invasive surgery: Hybrid image-guided surgery," *J. Pediatr. Surg.*, vol. 50, no. 1, pp. 30–36, 2015.

[3] M. I. Posner, M. J. Nissen, and R. M. Klein, "Visual dominance: An information-processing account of its origins and significance," *Psychol. Rev.*, vol. 83, no. 2, pp. 157–171, 1976.

[4] Y. Dai *et al.*, "Biaxial sensing suture breakage warning system for robotic surgery," *Biomed. Microdevices*, vol. 21, no. 1, 2019, Art. no. 10, [Online]. Available: https://link.springer.com/article/10.1007/s10544-018-0357-6

[5] P. J. Johnson, D. E. Schmidt, and U. Duvvuri, "Output control of da vinci surgical system's surgical graspers," *J. Surg. Res.*, vol. 186, no. 1, pp. 56–62, 2014.

[6] R. Bogue, "Robots in healthcare," *Ind. Robot: An Int. J.*, vol. 38, no. 3, pp. 218–223, 2011.

[7] A. Abiri *et al.*, "Suture breakage warning system for robotic surgery," *IEEE Trans. Biomed. Eng.*, vol. 66, no. 4, pp. 1165–1171, Apr. 2019.

[8] M. E. Currie *et al.*, "The role of visual and direct force feedback in robotics-assisted mitral valve annuloplasty," *Int. J. Med. Robot. Comput. Assist. Surg.*, vol. 13, no. 3, 2017, Art. no. e1787.

[9] A. Torabi, K. Khadem, K. Zareinia, G. R. Sutherland, and M. Tavakoli, "Application of a redundant haptic interface in enhancing soft-tissue stiffness discrimination," *IEEE Robot. Automat. Lett.*, vol. 4, no. 2, pp. 1037–1044, Apr. 2019.

[10] J. Park, W. R. Provancher, and H. Z. Tan, "Haptic perception of edge sharpness in real and virtual environments," *IEEE Trans. Haptics*, vol. 10, no. 1, pp. 54–62, Jan.–Mar. 2016.

[11] W. J. Yoon, W.-Y. Hwang, and J. C. Perry, "Study on effects of effects of surface properties in haptic perception of virtual curvature," *Int. J. Comput. Appl. Technol.*, vol. 53, no. 3, pp. 236–243, 2016.

[12] M. O. Ernst and M. S. Banks, "Humans integrate visual and haptic information in a statistically optimal fashion," *Nature*, vol. 415, no. 6870, pp. 429–433, Jan. 2002.

[13] D. H. Lee, U. Kim, T. Gulrez, W. J. Yoon, B. Hannaford, and H. R. Choi, "A laparoscopic grasping tool with force sensing capability," *IEEE/ASME Trans. Mechatronics*, vol. 21, no. 1, pp. 130–141, Feb. 2016.

[14] F. Alambeigi, Z. Wang, R. Hegeman, Y. Liu, and M. Armand, "Autonomous data-driven manipulation of unknown anisotropic deformable tissues using unmodelled continuum manipulators," *IEEE Robot. Automat. Lett.*, vol. 4, no. 2, pp. 254–261, Apr. 2019.

[15] N. Herzig, P. Maiolino, F. Iida, and T. Nanayakkara, "A variable stiffness robotic probe for soft tissue palpation," *IEEE Robot. Automat. Lett.*, vol. 3, no. 2, pp. 1168–1175, Apr. 2018.

[16] X. Yu, H. J. Chizeck, and B. Hannaford, "Comparison of transient performance in the control of soft tissue grasping," in *Proc. IEEE/RSJ Int. Conf. Intell. Robots Syst.*, 2007, pp. 1809–1814.

[17] J.-J. Cabibihan, M. K. Abubasha, and K. Sadasivuni, "Recovery behavior of artificial skin materials after object contact," in *Proc. Int. Conf. Social Robot.*, 2016, pp. 449–457.

[18] T. Gulrez and W. J. Yoon, "Cutaneous haptic feedback system and methods of use," U.S. Patent 9946350 B2, Apr. 17, 2018.

[19] M. R. Afzal, H.-Y. Byun, M.-K. Oh, and J. Yoon, "Effects of kinesthetic haptic feedback on standing stability of young healthy subjects and stroke patients," *J. Neuroengineering Rehabil.*, vol. 12, 2015, Art. no. 27, [Online]. Available: https://link.springer.com/article/10.1007/s10544-018-0357-6

[20] H. Lee, B. Cheon, M. Hwang, D. Kang, and D.-S. Kwon, "A master manipulator with a remote-center-of-motion kinematic structure for a minimally invasive robotic surgical system," *Int. J. Med. Robot. Comput. Assist. Surg.*, vol. 14, no. 1, 2018, Art. no. e1865.

[21] S. McKinley *et al.*, "A single-use haptic palpation probe for locating subcutaneous blood vessels in robot-assisted minimally invasive surgery," in *Proc. IEEE Int. Conf. Automat. Sci. Eng.*, Aug. 2015, pp. 1151–1158.

[22] A. Y. Alhaddad *et al.*, "Toward 3D printed prosthetic hands that can satisfy psychosocial needs: Grasping force comparisons between a prosthetic hand and human hands," in *Proc. Int. Conf. Social Robot.*, 2017, pp. 304–313.

[23] J.-J. Cabibihan, D. Joshi, Y. Srinivasa, M. Chan, and A. Muruganantham, "Illusory sense of human touch from a warm and soft artificial hand," *IEEE Trans. Neural Syst. Rehabil. Eng.*, vol. 23, no. 3, pp. 517–527, May 2015.

[24] J.-J. Cabibihan, M. K. Abubasha, and N. Thakor, "A method for 3-D printing patient-specific prosthetic arms with high accuracy shape and size," *IEEE Access*, vol. 6, pp. 25029–25039, 2018.

[25] T. Sun, J. Back, and H. Liu, "Combining contact forces and geometry to recognize objects during surface haptic exploration," *IEEE Robot. Automat. Lett.*, vol. 3, no. 3, pp. 2509–2514, Jul. 2018.

[26] C. Gaudeni, M. Pozzi, Z. Iqbal, M. Malvezzi, and D. Prattichizzo, "Grasping with the softpad, a soft sensorized surface for exploiting environmental constraints with rigid grippers," *IEEE Robot. Automat. Lett.*, vol. 5, no. 3, pp. 3884–3891, Jul. 2020.

[27] H. Marcus *et al.*, "Forces exerted during microneurosurgery: A cadaver study," *Int. J. Med. Robot. Comput. Assist. Surg.*, vol. 10, pp. 251–256, 2014.

[28] G. Wetherill and H. Levitt, "Sequential estimation of points on a psychometric function," *Brit. J. Math. Stat. Psychol.*, vol. 18, no. 1, pp. 1–10, 1965.

[29] J.-J. Cabibihan, A. Y. Alhaddad, T. Gulrez, and W. J. Yoon, "Dataset for influence of visual and haptic feedback on the detection of threshold forces in a surgical grasping task," *IEEE DataPort*, Jan. 5, 2021. doi: 10.21227/apgp-3x82.

[30] S. Sokhanvar, J. Dargahi, S. Najarian, and S. Arbatani, *Bulk Softness Measurement Using A Smart Endoscopic Grasper*. Hoboken, NJ, USA: Wiley, 2012, ch. 5, pp. 99–111.

[31] H. Kang and J. T. Wen, "Autonomous suturing using minimally invasive surgical robots," in *Proc. IEEE Int. Conf. Control Appl. Conf.*, 2000, pp. 742–747.

[32] J. J. Cabibihan, S. Pattofatto, M. Jomaa, A. Benallal, M. C. Carrozza, and P. Dario, "The conformance test for robotic/prosthetic fingertip skins," in *Proc. IEEE/RAS-EMBS Int. Conf. Biomed. Robot. Biomechatronics* 2006, pp. 561–566.

[33] Y.-J. Lim, D. Deo, T. P. Singh, D. B. Jones, and S. De, "In situ measurement and modeling of biomechanical response of human cadaveric soft tissues for physics-based surgical simulation," *Surg. Endoscopy*, vol. 23, no. 6, 2009, Art. no. 1298.

[34] N. Enayati, E. De Momi, and G. Ferrigno, "Haptics in robot-assisted surgery: Challenges and benefits," *IEEE Rev. Biomed. Eng.*, vol. 9, pp. 49–65, Mar. 2016, doi: 10.1109/rbme.2016.2538080.

[35] L. C. García-Peraza-Herrera *et al.*, "Toolnet: Holistically-nested real-time segmentation of robotic surgical tools," in *Proc. IEEE/RSJ Int. Conf. Intell. Robots Syst.*, Sep. 2017, pp. 5717–5722.

[36] S. J. Lederman and R. L. Klatzky, "Hand movements: A window into haptic object recognition," *Cogn. Psychol.*, vol. 19, no. 3, pp. 342–368, 1987.

[37] K. Drewing, T. V. Wiecki, and M. O. Ernst, "Material properties determine how force and position signals combine in haptic shape perception," *Acta Psychologica*, vol. 128, no. 2, pp. 264–273, 2008.

[38] R. A. Jacobs, "What determines visual cue reliability?," *Trends Cogn. Sci.*, vol. 6, no. 8, pp. 345–350, 2002.

[39] M. Korman, K. Teodorescu, A. Cohen, M. Reiner, and D. Gopher, "Effects of order and sensory modality in stiffness perception," *Teleoperators Virtual Environments - Presence*, vol. 21, pp. 295–304, Aug. 2012.

[40] A. Abiri *et al.*, "Multi-modal haptic feedback for grip force reduction in robotic surgery," *Sci. Reports*, vol. 9, no. 1, 2019, Art. no. 5016.

[41] S. Greenish, V. Hayward, V. Chial, A. Okamura, and T. Steffen, "Measurement, analysis, and display of haptic signals during surgical cutting," *Presence: Teleoperators Virtual Environments*, vol. 11, no. 6, pp. 626–651, Dec. 2002.